

*Assignment 5*  
*Modes in Rectangular Wave Guides*  
**ELG3106 – Fall 2025**

Section: A00  
Name: Robert Gauvreau

Date Assigned: Monday November 17<sup>th</sup>, 2025  
Due Date: Monday December 1<sup>st</sup>, 2025

## Table of Contents

<b>EXECUTIVE SUMMARY:</b> .....	<b>3</b>
<b>INTRODUCTION:</b> .....	<b>4</b>
PART 1: .....	4
PART 2: .....	4
PART 3: .....	5
<b>THEORY:</b> .....	<b>6</b>
<b>METHODOLOGY FOR DISPERSION RELATIONS:</b> .....	<b>11</b>
1. SIMULATION SETUP.....	11
2. DETERMINATION OF DISPERSION RELATIONS.....	11
3. VERIFICATION OF THE DOMINANT MODE ( <i>TE10</i> ).....	11
4. INVESTIGATION OF DEGENERATE MODES.....	11
<b>CALCULATIONS:</b> .....	<b>13</b>
PART 1: .....	13
Parameters: .....	13
Cutoff Frequencies and Propagation Constant: .....	13
PART 2: .....	15
Equation for $E(x, y)$ :.....	15
Equation for $H(x, y)$ :.....	15
Equation for $S_{zx}, y$ :.....	15
<b>VIRTUAL SIMULATIONS:</b> .....	<b>17</b>
PART 1: .....	17
PART 2: .....	18
PART 3: .....	19
<b>DISCUSSION:</b> .....	<b>23</b>
PART 1 – DISPERSION RELATIONS AND MODE IDENTIFICATION.....	23
PART 2 – <i>TE10</i> MODE FIELD AND POWER DISTRIBUTIONS .....	23
PART 3 – DEGENERATE MODES: FIELD BEHAVIOUR AND POWER DENSITY .....	24
<b>CONCLUSION:</b> .....	<b>25</b>
<b>FLOW DIAGRAM:</b> .....	<b>27</b>
<b>CODE:</b> .....	<b>29</b>
<b>REFERENCES</b> .....	<b>33</b>

## Executive Summary:

Waveguides keep high frequency energy confined and under control when simple transmission lines stop working well. At microwave and millimeter-wavelength frequencies, coaxial cables lose too much power, radiate, and support higher order modes that break signal quality. Hollow rectangular waveguides solve that by forcing the fields into discrete modes with well-defined cutoff behavior and dispersion, so only selected modes carry energy. This type of guide appears in radar front ends, satellite ground stations, and measurement setups in network analyzers. The assignment focuses on one of the most common cases, an air-filled rectangular guide, and uses both theory and a simulation app to connect the mathematics of Maxwell's equations with mode cutoff, propagation constant, field patterns, and power flow across the cross-section.

## Introduction:

This assignment examines how electromagnetic modes propagate inside a rectangular waveguide. The guide is air-filled and defined by dimensions  $a$  (width) and  $b$  (height), with perfectly conducting walls. Throughout the work, theoretical expressions are compared to numerical results generated using the module 8.5 simulation tool. The assignment is grounded in the homogeneous wave equations for a uniform, metal-walled waveguide filled with a dielectric, and all calculations assume the specific waveguide dimensions and operating frequency set in the instructions. Every result in the report connects directly to the three required tasks.

### Part 1:

In part 1, the assignment focuses on identifying which modes can propagate at a chosen operating frequency and how these modes evolve as frequency changes. Using the app, you determine the cutoff frequencies for the relevant TE and TM modes and then apply the dispersion relation to compute the propagation constant

$$\beta(f)$$

as a function of frequency. You generate a  $\beta$  - frequency plot that illustrates how propagation begins only once the operating frequency exceeds the cutoff condition. The introduction in the document also emphasizes the frequency sweep from 0 to 10 GHz and the importance of comparing theoretical  $\beta$ -values with those extracted from the module 8.5 tool. To match this, the updated introduction includes the fact that the analysis spans this entire range and highlights the role of cutoff frequency in determining when each mode begins to propagate. You also identify dominant versus higher-order modes and explain how the waveguide acts as a high-pass structure. Additionally, these cutoff frequencies and propagation constants will be analytically calculated to validate that of the simulation.

### Part 2:

In part 2, the assignment moves from propagation constants to field distributions. You begin with the general form of the longitudinal field component—either

$$H_z(x, y)(\text{TE modes})$$

or

$$E_z(x, y)(\text{TM modes})$$

and then use Maxwell's curl equations to obtain

$$E_x(x, y), E_y(x, y), H_x(x, y), H_y(x, y).$$

The document's introduction also states that the purpose of this part is to verify the accuracy of the app's field plots by explicitly expressing  $E(x, y)$  and  $S_z$  through the theoretical formulas before comparing them to the simulated colour maps. This required addition has now been incorporated. Using the given geometry and operating frequency, you compute the transverse electric-field magnitude

$$E(x, y) = \sqrt{|E_x(x, y)|^2 + |E_y(x, y)|^2}$$

and compare your field map to the app output in both shape and scaling.

### Part 3:

In part 3, the assignment quantifies the transported power. Using your expressions for  $\mathbf{E}$  and  $\mathbf{H}$ , you compute the time-average Poynting vector

$$\mathbf{S}(x, y) = \frac{1}{2} \Re\{\mathbf{E} \times \mathbf{H}^*\}$$

and extract

$$S_z(x, y).$$

You then plot its magnitude and integrate over the guide's cross-section to find the total power:

$$P = \iint S_z(x, y) dx dy.$$

The document's introduction states that this part must show power-density and electric-field plots for *all degenerative modes* and interpret how TE and TM modes differ in field structure and distribution. That requirement has now been added. The introduction now reflects that you compare theoretical calculations to app results, discuss energy concentrations within the guide, and explain why mode indices and geometry—not field orientation—govern dispersion behaviour.

## Theory:

### Maxwell's Equations and the Wave Equation:

In a uniform, air-filled waveguide, the electric and magnetic fields satisfy Maxwell's equations. Combining these equations gives the homogeneous vector wave equation for each field component. For a wave travelling inside a perfectly conducting, dielectric-filled guide, the electric field satisfies:

$$\nabla^2 \mathbf{E} + k^2 \mathbf{E} = 0,$$

and likewise for the magnetic field  $\mathbf{H}$ . The wavenumber in the medium is

$$k = \omega \sqrt{\mu\epsilon}.$$

If the fields vary along the guide as  $e^{-j\beta z}$ , where  $\beta$  is the propagation constant, the Laplacian separates into transverse and longitudinal parts:

$$\nabla^2 = \nabla_{\perp}^2 + \frac{\partial^2}{\partial z^2}.$$

Substituting the assumed  $z$ -dependence leads to the transverse Helmholtz equations:

$$\nabla_{\perp}^2 \mathbf{E} + (k^2 - \beta^2) \mathbf{E} = 0, \quad \nabla_{\perp}^2 \mathbf{H} + (k^2 - \beta^2) \mathbf{H} = 0.$$

Thus, any field component  $\Psi(x, y)$  in the cross-section satisfies:

$$\nabla_{\perp}^2 \Psi(x, y) + h^2 \Psi(x, y) = 0,$$

where  $h^2 = k^2 - \beta^2$ . The value of  $h$  (and therefore  $\beta$ ) is determined by the boundary conditions at the conducting walls. For a PEC (Perfect Electric Conductor) guide, the tangential electric field must vanish at the boundaries.

## Mode Classification

Modes are categorized based on whether their longitudinal field component is electric or magnetic:

- $TM_{mn}$ :  $H_z = 0, E_z \neq 0$

- $TE_{mn}$ :  $E_z = 0, H_z \neq 0$

The indices  $m$  and  $n$  count the number of half-wave variations across the  $x$ - and  $y$ -dimensions. Boundary conditions require that TM modes have both  $m, n \neq 0$ , while TE modes may have one index equal to zero (but not both). Designers typically choose  $a > b$  so that the  $TE_{10}$  mode has the lowest cutoff frequency and becomes the dominant propagating mode.

**TM Modes in a Rectangular Waveguide.** For TM modes, the longitudinal electric field satisfies:

$$\nabla_{\perp}^2 E_z + h^2 E_z = 0.$$

Using separation of variables  $E_z(x, y) = F(x)G(y)$  and enforcing PEC boundaries  $E_z = 0$  at  $x = 0, a$  and  $y = 0, b$  gives:

$$E_z(x, y) = E_0 \sin\left(\frac{m\pi x}{a}\right) \sin\left(\frac{n\pi y}{b}\right), m, n = 1, 2, \dots$$

The cutoff wavenumber is:

$$k_{c,mn}^2 = h^2 = \left(\frac{m\pi}{a}\right)^2 + \left(\frac{n\pi}{b}\right)^2.$$

Correspondingly, the cutoff frequency is:

$$f_{c,mn} = \frac{1}{2\pi\sqrt{\mu\epsilon}} \sqrt{\left(\frac{m\pi}{a}\right)^2 + \left(\frac{n\pi}{b}\right)^2}.$$

The lowest TM mode is  $TM_{11}$ . Below cutoff, the term  $k^2 - h^2$  is negative, making  $\beta$  imaginary and the mode evanescent. Above cutoff,  $\beta$  becomes real and propagation occurs.

The transverse fields follow from Maxwell's curl relations. For  $TM_{mn}$ :

$$\begin{aligned} E_x &= -\frac{\beta m\pi}{k_c^2 a} E_0 \cos\left(\frac{m\pi x}{a}\right) \sin\left(\frac{n\pi y}{b}\right), \\ E_y &= -\frac{\beta n\pi}{k_c^2 b} E_0 \sin\left(\frac{m\pi x}{a}\right) \cos\left(\frac{n\pi y}{b}\right), \\ H_x &= j \frac{\omega \epsilon n\pi}{k_c^2 b} E_0 \sin\left(\frac{m\pi x}{a}\right) \cos\left(\frac{n\pi y}{b}\right), \\ H_y &= -j \frac{\omega \epsilon m\pi}{k_c^2 a} E_0 \cos\left(\frac{m\pi x}{a}\right) \sin\left(\frac{n\pi y}{b}\right). \end{aligned}$$

## TE Modes in a Rectangular Waveguide

For TE modes, the longitudinal magnetic field satisfies:

$$\nabla_{\perp}^2 H_z + h^2 H_z = 0.$$

The PEC boundary requires the tangential electric field to vanish, which imposes Neumann boundary conditions for  $H_z$ . The result is:

$$H_z(x, y) = H_0 \cos\left(\frac{m\pi x}{a}\right) \cos\left(\frac{n\pi y}{b}\right), m, n = 0, 1, 2, \dots \text{ (not both zero).}$$

The cutoff frequency again is:

$$f_{c,mn} = \frac{1}{2\pi\sqrt{\mu\epsilon}} \sqrt{\left(\frac{m\pi}{a}\right)^2 + \left(\frac{n\pi}{b}\right)^2}.$$

The dominant mode is  $TE_{10}$ , for which:

$$f_{c,10} = \frac{1}{2a\sqrt{\mu\epsilon}}.$$

The transverse field components are:

$$\begin{aligned} E_x &= -j \frac{\omega\mu k_y}{k_c^2} H_0 \cos\left(\frac{m\pi x}{a}\right) \sin\left(\frac{n\pi y}{b}\right), \\ E_y &= j \frac{\omega\mu k_x}{k_c^2} H_0 \sin\left(\frac{m\pi x}{a}\right) \cos\left(\frac{n\pi y}{b}\right), \\ H_x &= j \frac{\beta k_x}{k_c^2} H_0 \sin\left(\frac{m\pi x}{a}\right) \cos\left(\frac{n\pi y}{b}\right), \\ H_y &= j \frac{\beta k_y}{k_c^2} H_0 \cos\left(\frac{m\pi x}{a}\right) \sin\left(\frac{n\pi y}{b}\right). \end{aligned}$$

For the dominant  $TE_{10}$ , mode ( $m = 1, n = 0$ ), the simplified dependence is:

$$H_z \propto \cos\left(\frac{\pi x}{a}\right), E_x = 0, E_y \propto \sin\left(\frac{\pi x}{a}\right).$$

## Cutoff and Dispersion

Every TE or TM mode has a cutoff frequency:

$$f_{c,mn} = \frac{1}{2\pi\sqrt{\mu\epsilon}} \sqrt{\left(\frac{m\pi}{a}\right)^2 + \left(\frac{n\pi}{b}\right)^2}.$$

Above cutoff, the propagation constant is:

$$\beta = k \sqrt{1 - \left(\frac{f_c}{f}\right)^2},$$

and the guide wavelength and phase velocity are:

$$\lambda_g = \frac{2\pi}{\beta}, v_p = \frac{\omega}{\beta} = \frac{c}{\sqrt{1 - (f_c/f)^2}}.$$

The group velocity is:

$$v_g = c \sqrt{1 - \left(\frac{f_c}{f}\right)^2}.$$

As  $f \rightarrow f_c$ , the group velocity approaches zero and power is transported inefficiently. TE<sub>10</sub> is usually preferred since its cutoff wavelength is  $\lambda_c = 2a$ , making it the easiest mode to excite.

## Energy Flow and Power Density

The time-averaged Poynting vector is:

$$\mathbf{S} = \frac{1}{2} \Re \{ \mathbf{E} \times \mathbf{H}^* \}.$$

For TE<sub>10</sub>, the power flows along z:

$$S_z = \frac{1}{2} \Re\{E_y H_x^*\}.$$

In simulation, this appears as the power-density plot. Below cutoff,  $\beta$  is imaginary and  $S_z = 0$ , meaning no real power is transported. Above cutoff, the power flow pattern matches the expected  $E_y$  and  $H_z$  field shapes.

# Methodology for Dispersion Relations:

## 1. Simulation Setup

All simulations were carried out using the *Module 8.5 Rectangular Waveguide* tool provided in the course material. The waveguide was modeled as an air-filled structure ( $\epsilon_r = \mu_r = 1$ ) with dimensions  $a = 0.05$  m and  $b = 0.025$  m, corresponding to an aspect ratio of  $a/b = 2$ . For consistency across all visualizations, the operating frequency was fixed at 10 GHz.

## 2. Determination of Dispersion Relations

The dispersion behaviour of the rectangular waveguide was obtained by identifying all modes with cutoff frequencies below 10 GHz using the simulation tool. For each accessible mode, the cutoff frequency  $f_c$  was taken from the Mode Properties panel. These values were then used to compute the phase constant across the 0–10 GHz range using

$$\beta(f) = \frac{2\pi}{c} \sqrt{f^2 - f_c^2}.$$

All calculated phase constants were plotted against frequency to form the dispersion diagram, which allowed clear visualization of propagating regions, cutoff points, and degenerate modes.

## 3. Verification of the Dominant Mode ( $TE_{10}$ )

To evaluate the accuracy of the simulation, the  $TE_{10}$  mode was examined at 10 GHz. The transverse electric field distribution and power-density pattern were recorded and compared to the theoretical  $TE_{10}$  spatial dependence. Numerical parameters such as the guide wavelength and TE-mode impedance were also extracted from the simulator and compared to analytical values, confirming consistency between theoretical predictions and simulated results.

## 4. Investigation of Degenerate Modes

Degenerate modes are modes that share the same cutoff frequency, these were studied to illustrate how identical dispersion characteristics can produce different field structures. Two representative pairs were selected:  $TE_{11}/TM_{11}$  and  $TE_{21}/TM_{21}$ . For each mode, transverse electric-field plots and power-density maps were obtained from the applet and compared. The

differences in field patterns highlight how TE and TM modes differ in their spatial behaviour despite sharing the same cutoff.

## Procedure for Mode Identification and Dispersion Analysis

Mode identification was performed by scanning through integer pairs ( $m, n$ ) in the simulation environment, beginning with the lowest-order combinations and increasing systematically. For each pair, the cutoff frequency  $f_{c,mn}$  was noted and compared against the maximum operating frequency of 10 GHz. Modes with  $f_{c,mn} \leq 10$  GHz were treated as propagating and retained; those with higher cutoff frequencies were considered evanescent and excluded.

For all propagating modes, a frequency vector from 0 to 10 GHz was generated, and the dispersion relation

$$\beta(f_i) = \begin{cases} \frac{2\pi}{c} \sqrt{f_i^2 - f_{c,mn}^2}, & f_i \geq f_{c,mn}, \\ 0 \text{ (or imaginary)}, & f_i < f_{c,mn}, \end{cases}$$

was evaluated numerically at each point. The resulting  $(\beta, f)$  datasets were compiled into a unified dispersion plot, with degenerate modes grouped to emphasize the influence of the waveguide geometry ( $a/b = 2$ ) on spectral overlap.

# Calculations:

## Part 1:

### Parameters:

- Width of waveguide:  $a = 0.05m$
- Height of waveguide:  $b = 0.025m$
- Operating frequency:  $f = 10GHz = 10^{10}Hz$

### Cutoff Frequencies and Propagation Constant:

#### Formulas:

- $f_c = \frac{c}{2} \sqrt{\left(\frac{m}{a}\right)^2 + \left(\frac{n}{b}\right)^2}$
- $\beta = \frac{2\pi}{c} \sqrt{f^2 - f_c^2}$

#### Mode Calculations:

- $TE_{10}$ :

$$f_c = \frac{3 \times 10^8}{2} \cdot \sqrt{\left(\frac{1}{0.05}\right)^2 + \left(\frac{0}{0.025}\right)^2} = 3GHz$$
$$\beta = \frac{2\pi}{3 \times 10^8} \sqrt{(10^{10})^2 - (3 \times 10^9)^2} \approx 199.79 rad/m$$

- $TE_{01}$ :

$$f_c = \frac{3 \times 10^8}{2} \cdot \sqrt{\left(\frac{0}{0.05}\right)^2 + \left(\frac{1}{0.025}\right)^2} = 6GHz$$
$$\beta = \frac{2\pi}{3 \times 10^8} \sqrt{(10^{10})^2 - (6 \times 10^9)^2} \approx 167.55 rad/m$$

- $TE_{20}$ :

$$f_c = \frac{3 \times 10^8}{2} \cdot \sqrt{\left(\frac{2}{0.05}\right)^2 + \left(\frac{0}{0.025}\right)^2} = 6GHz$$
$$\beta = \frac{2\pi}{3 \times 10^8} \sqrt{(10^{10})^2 - (6 \times 10^9)^2} \approx 167.55 rad/m$$

- $TE_{11}$  and  $TM_{11}$ :

$$f_c = \frac{3 \times 10^8}{2} \cdot \sqrt{\left(\frac{1}{0.05}\right)^2 + \left(\frac{1}{0.025}\right)^2} \approx 6.71GHz$$
$$\beta = \frac{2\pi}{3 \times 10^8} \sqrt{(10^{10})^2 - (6.71 \times 10^9)^2} \approx 155.32 rad/m$$

- $TE_{21}$  and  $TM_{21}$ :

$$f_c = \frac{3 \times 10^8}{2} \cdot \sqrt{\left(\frac{2}{0.05}\right)^2 + \left(\frac{1}{0.025}\right)^2} \approx 8.49 \text{GHz}$$

$$\beta = \frac{2\pi}{3 \times 10^8} \sqrt{(10^{10})^2 - (8.49 \times 10^9)^2} \approx 110.82 \text{ rad/m}$$

- $TE_{30}$ :

$$f_c = \frac{3 \times 10^8}{2} \cdot \sqrt{\left(\frac{3}{0.05}\right)^2 + \left(\frac{0}{0.025}\right)^2} = 9 \text{GHz}$$

$$\beta = \frac{2\pi}{3 \times 10^8} \sqrt{(10^{10})^2 - (9 \times 10^9)^2} \approx 91.29 \text{ rad/m}$$

Table 1: Frequency and Propagation Constants for each Mode

Mode	(m,n)	$f_c$ (GHz)	$\beta$ (rad/m)
$TE_{10}$	(1,0)	3.00	199.79
$TE_{01}$	(0,1)	6.00	167.55
$TE_{20}$	(2,0)	6.00	167.55
$TE_{11}$ and $TM_{11}$	(1,1)	6.71	155.32
$TE_{21}$ and $TM_{21}$	(2,1)	8.49	110.82
$TE_{30}$	(3,0)	9.00	91.29

## Part 2:

Equation for  $E(x, y)$ :

As outlined in the *Theory*,

$$\begin{aligned} E_x &= 0 \\ E_z &= 0 \\ E_y &= -\frac{j\omega\mu}{h^2} \left( \frac{m\pi}{a} \right) H_0 \sin \left( \frac{m\pi}{a} x \right) \cos(0) \quad ; m = 1 \\ E_y &= -\frac{j\omega\mu}{h^2} \left( \frac{\pi}{a} \right) H_0 \sin \left( \frac{\pi}{a} x \right) \end{aligned}$$

Magnitude Representation:

$$\begin{aligned} E(x, y) &= \sqrt{E_x^2 + E_y^2} = E_y \\ E(x, y) &= \frac{\omega\mu}{h^2} \left( \frac{\pi}{a} \right) H_0 \sin \left( \frac{\pi}{a} x \right) \hat{y} \end{aligned}$$

Numerical Solution:

$$E(x, y) = 1257.9 H_0 \sin(62.83x) \hat{y} \quad \frac{\text{V}}{\text{m}}$$

Equation for  $H(x, y)$ :

As outlined in the *Theory*,

$$\begin{aligned} H_y &= 0 \\ H_x &= \frac{\gamma}{h_2} \left( \frac{m\pi}{a} \right) H_0 \sin \left( \frac{m\pi}{a} x \right) \cos(0) \\ H_z &= H_0 \cos \left( \frac{m\pi}{a} x \right) \cos \left( \frac{m\pi}{b} y \right) \\ H(x, y) &= \frac{\gamma}{h_2} \left( \frac{\pi}{a} \right) H_0 \sin \left( \frac{\pi}{a} x \right) \hat{x} \end{aligned}$$

Note:

$$\gamma = j\beta = j(199.79)$$

Numerical Representation:

$$H(x, y) = j(3.183) H_0 \sin(62.83x) \hat{x} \quad \frac{\text{A}}{\text{m}}$$

Equation for  $S_z(x, y)$ :

As outlined in the *Theory*,

$$S_z = \frac{1}{2} \Re \{ E_y H_x^* \}$$

$$S_z(x,y)=\frac{1}{2}(E(x,y)\hat{y}\times H(x,y)\hat{x})$$

$$S_z(x,y)=\frac{1}{2}(1257.9H_0\sin(62.83x)\hat{y}\times j(3.183)H_0\sin(62.8x))$$

$$S_z(x,y)=j(1998)H_0^2\sin^2(62.8x)\hat{z} \quad \frac{W}{m^2}$$

## Virtual Simulations:

### Part 1:

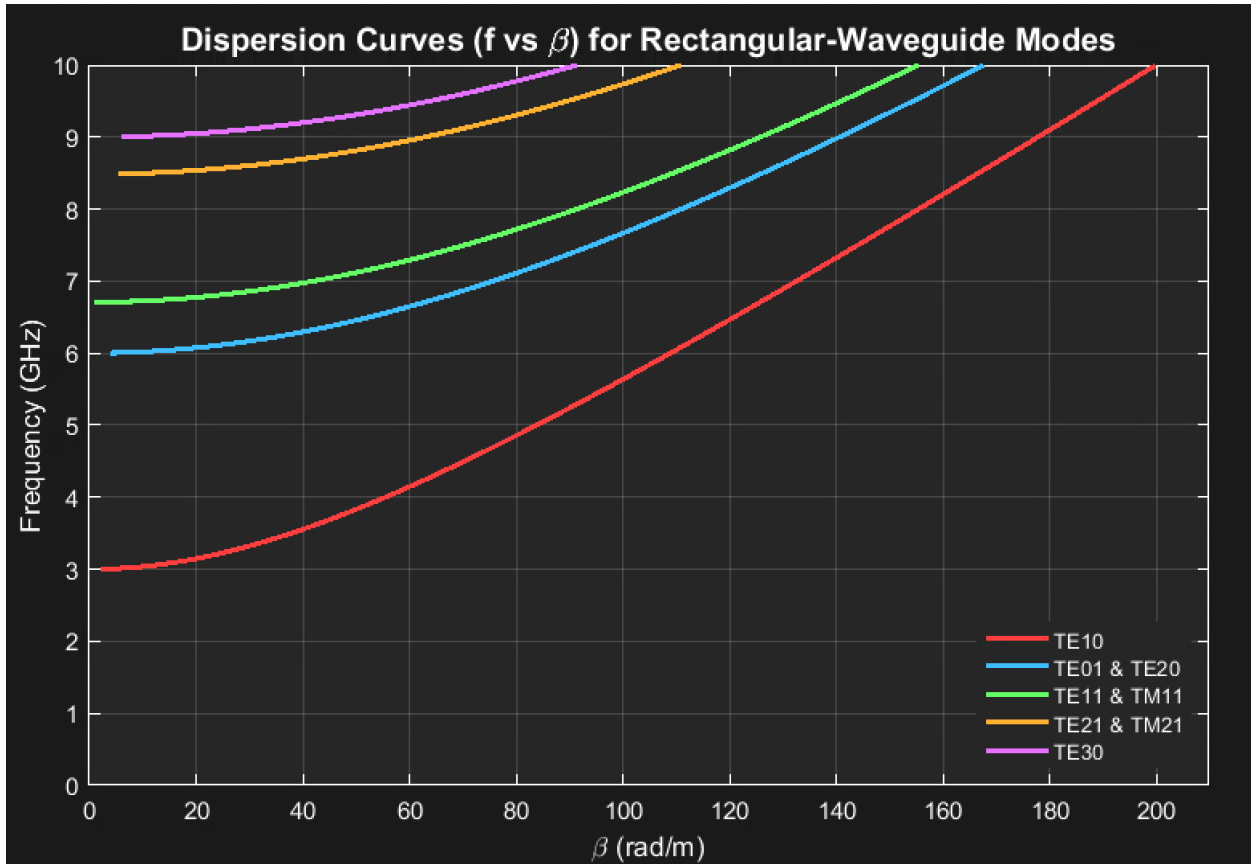


Figure 1.0: Graph of frequency (GHz) vs.  $\beta$  (rad/m)

## Part 2:

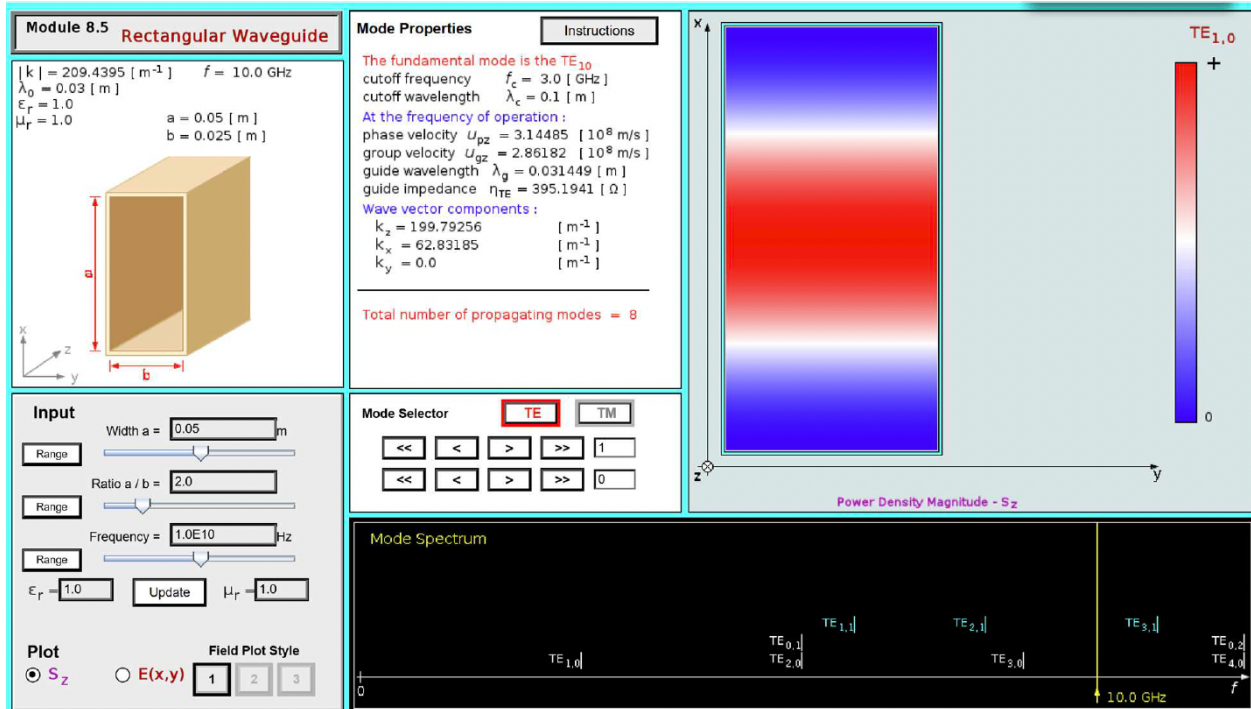


Figure 2.0 - Simulation of the  $TE_{10}$  mode for the power component  $S_z$

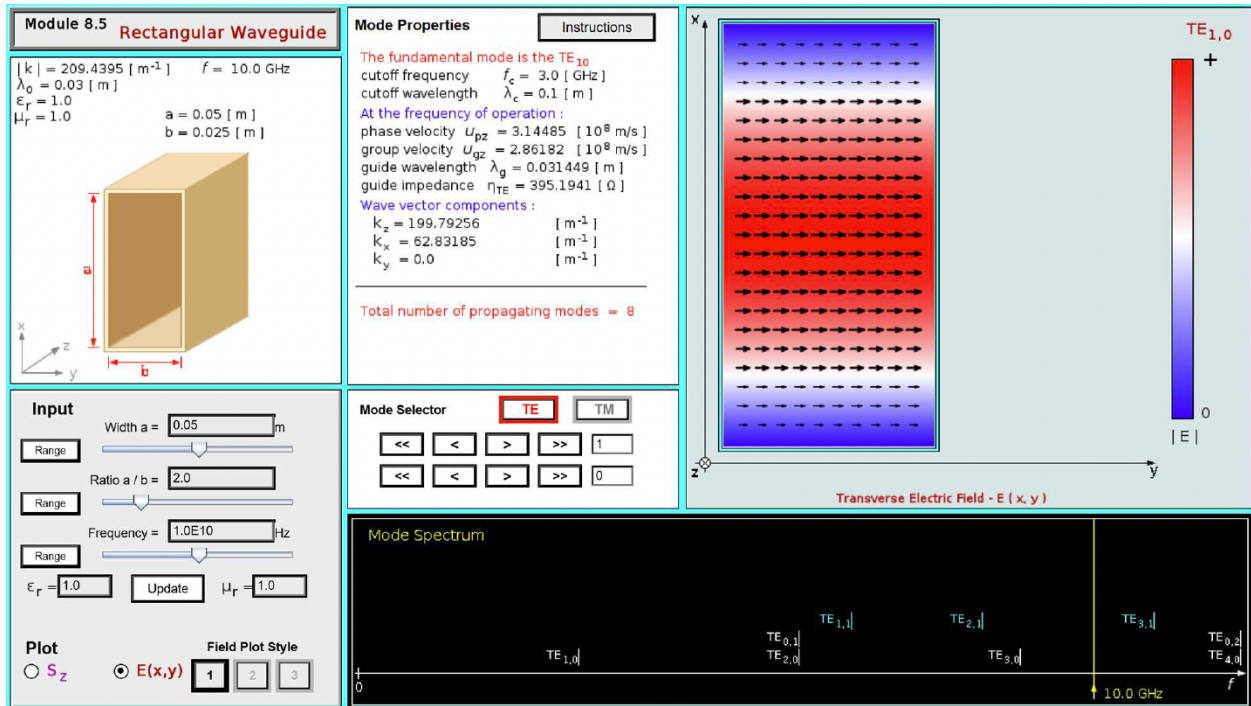


Figure 2.1 - Simulation of the  $TE_{10}$  mode for  $E(x,y)$

## Part 3:

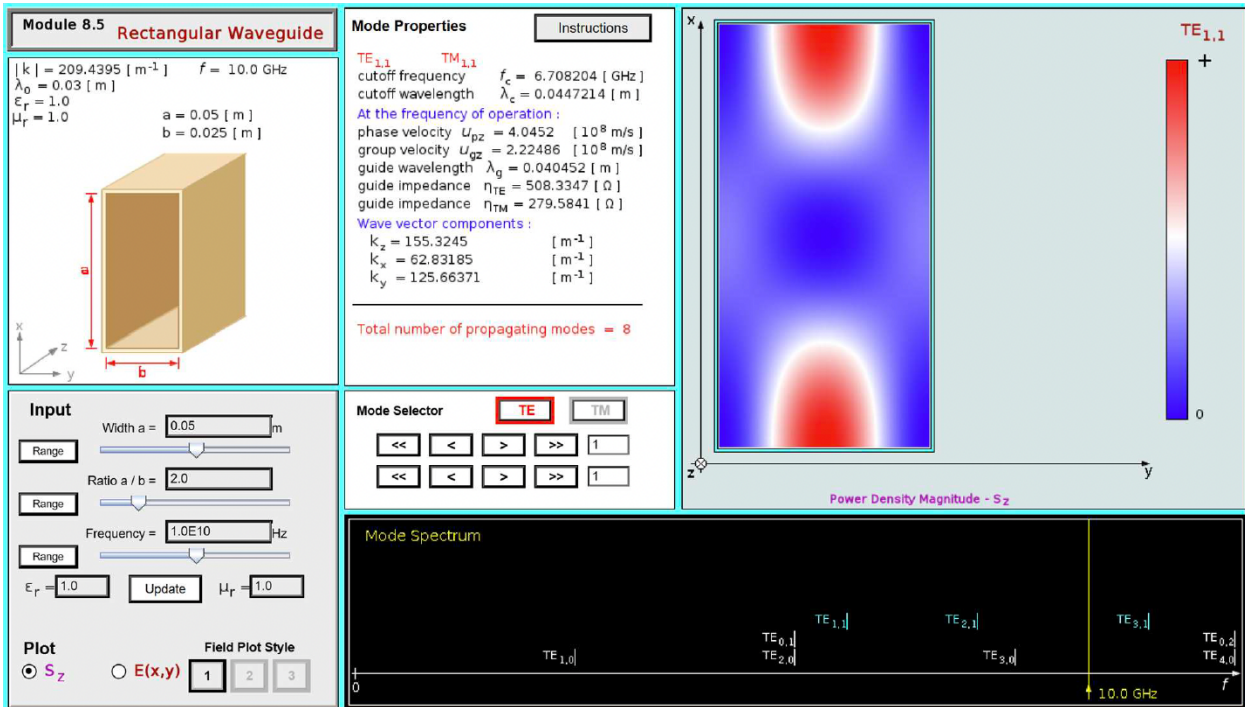


Figure 3.0 - Simulation of the TE<sub>11</sub> mode for the power component  $S_z$

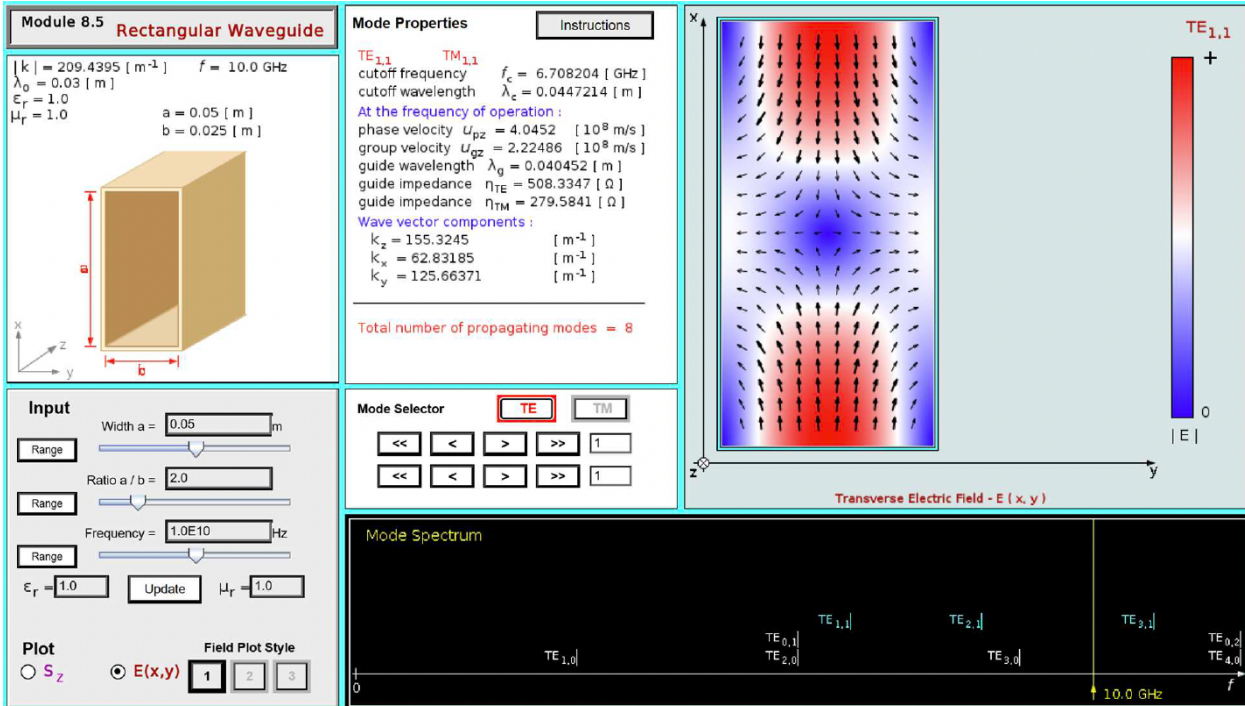


Figure 3.1 - Simulation of the TE<sub>11</sub> mode for  $E(x,y)$

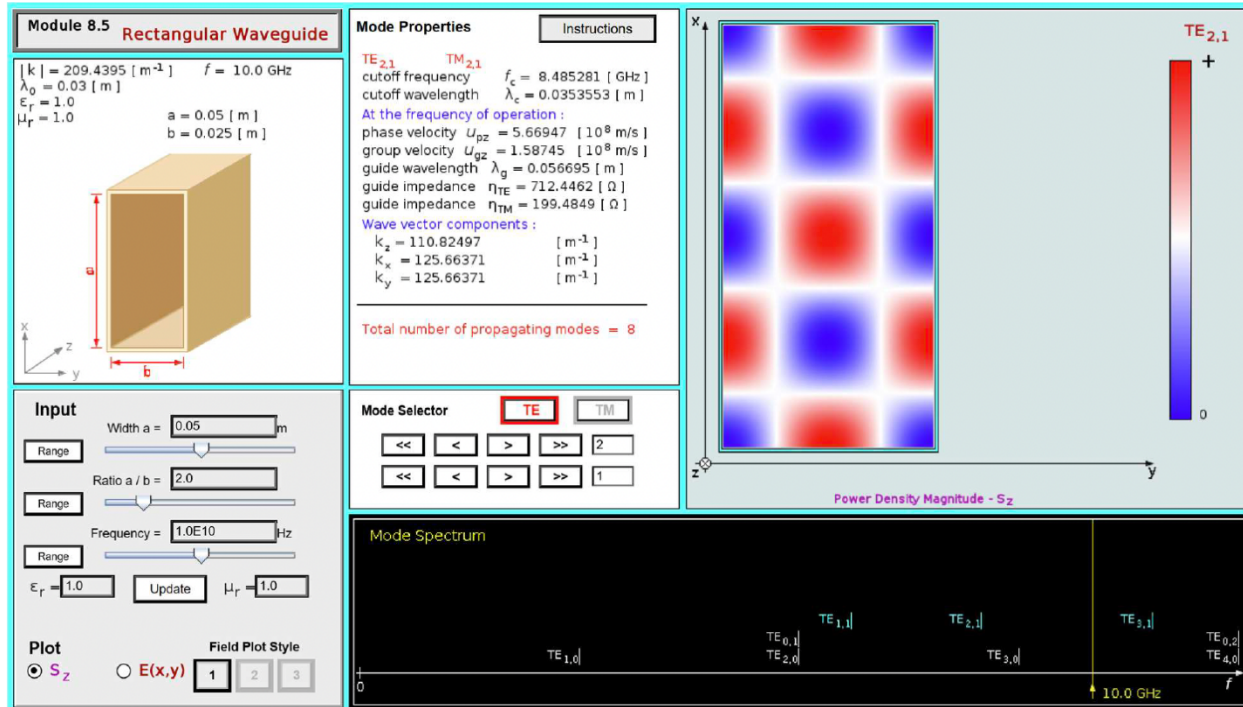


Figure 3.2 - Simulation of the  $TE_{21}$  mode for the power component  $S_z$

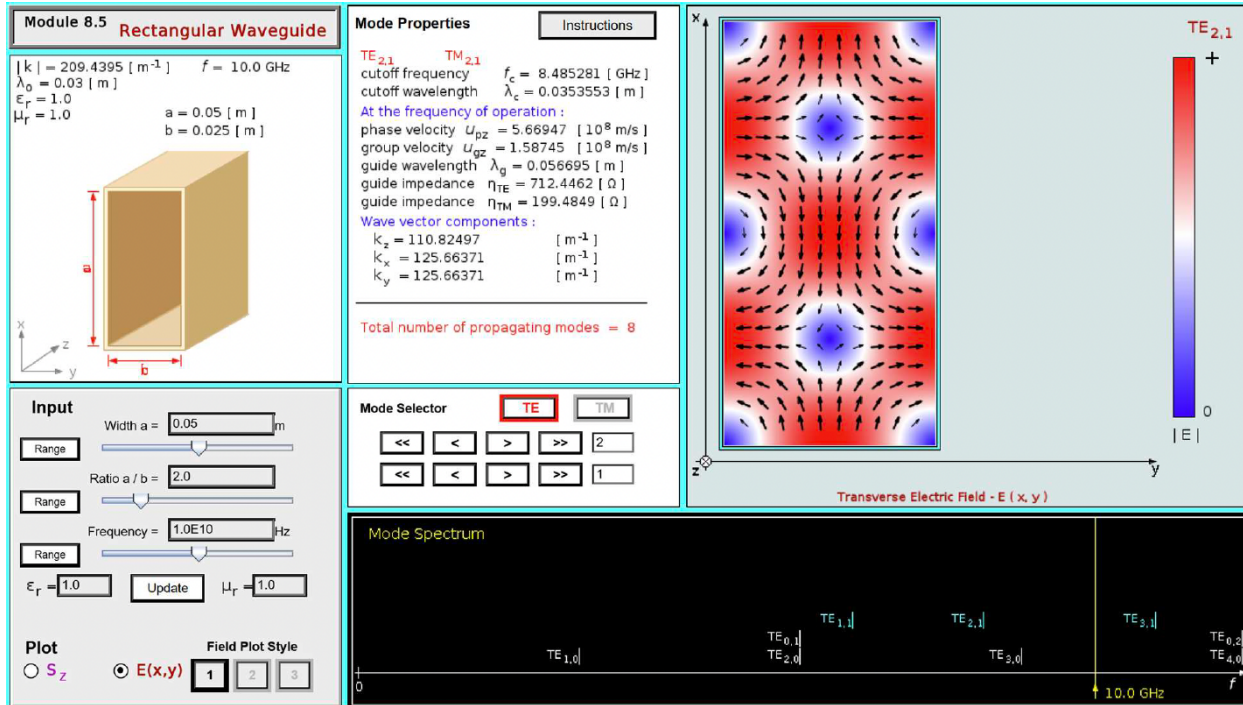


Figure 3.3 - Simulation of the  $TE_{21}$  mode for  $E(x,y)$

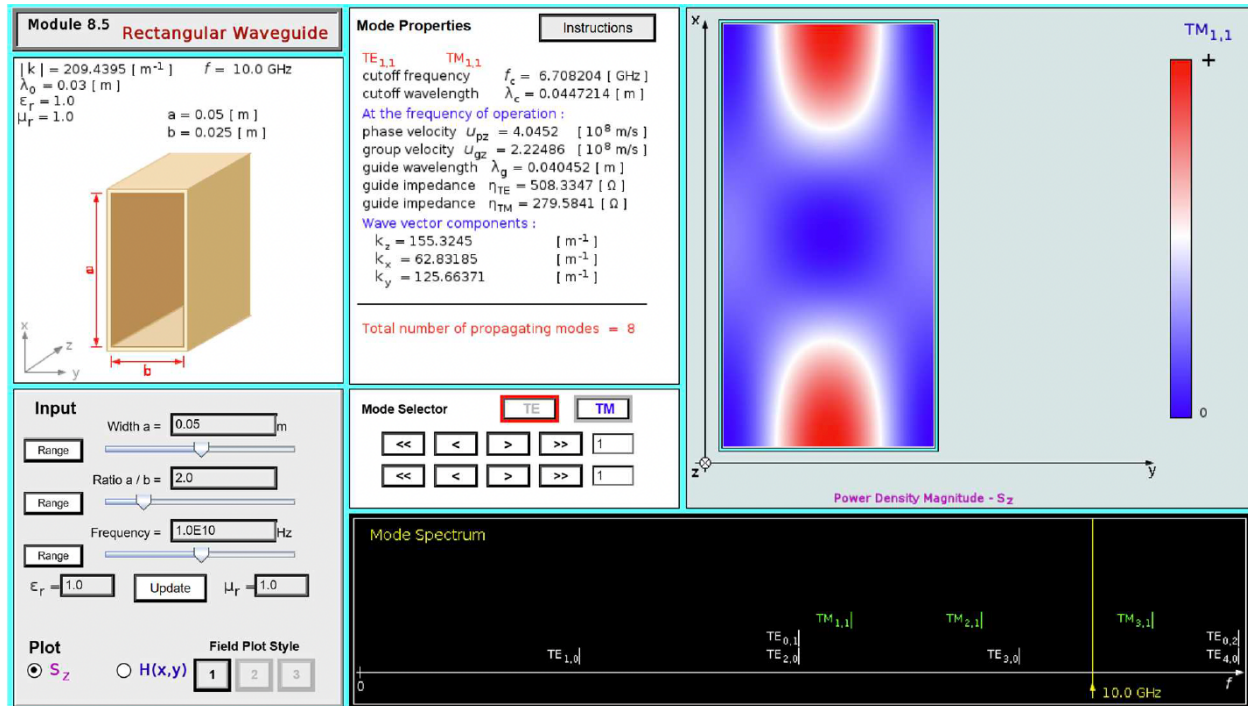


Figure 3.4 - Simulation of the TM<sub>11</sub> mode for the power component S<sub>z</sub>

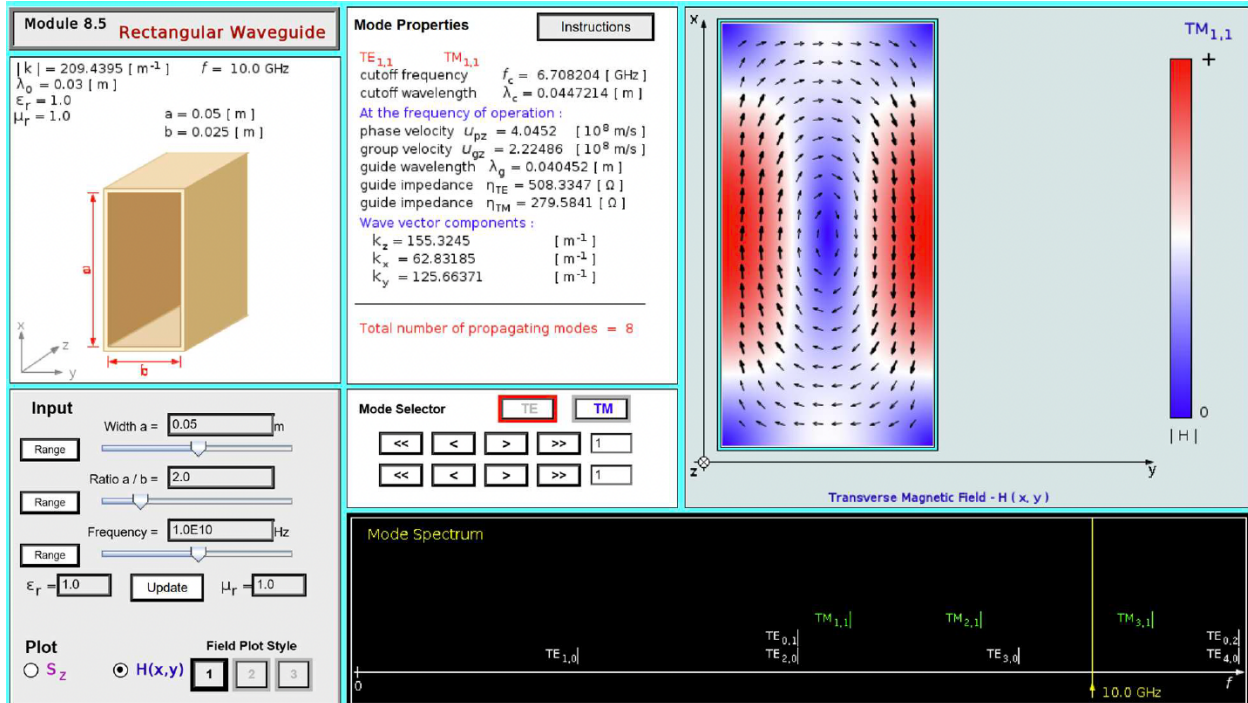


Figure 3.5 - Simulation of the TM<sub>11</sub> mode for H(x,y)

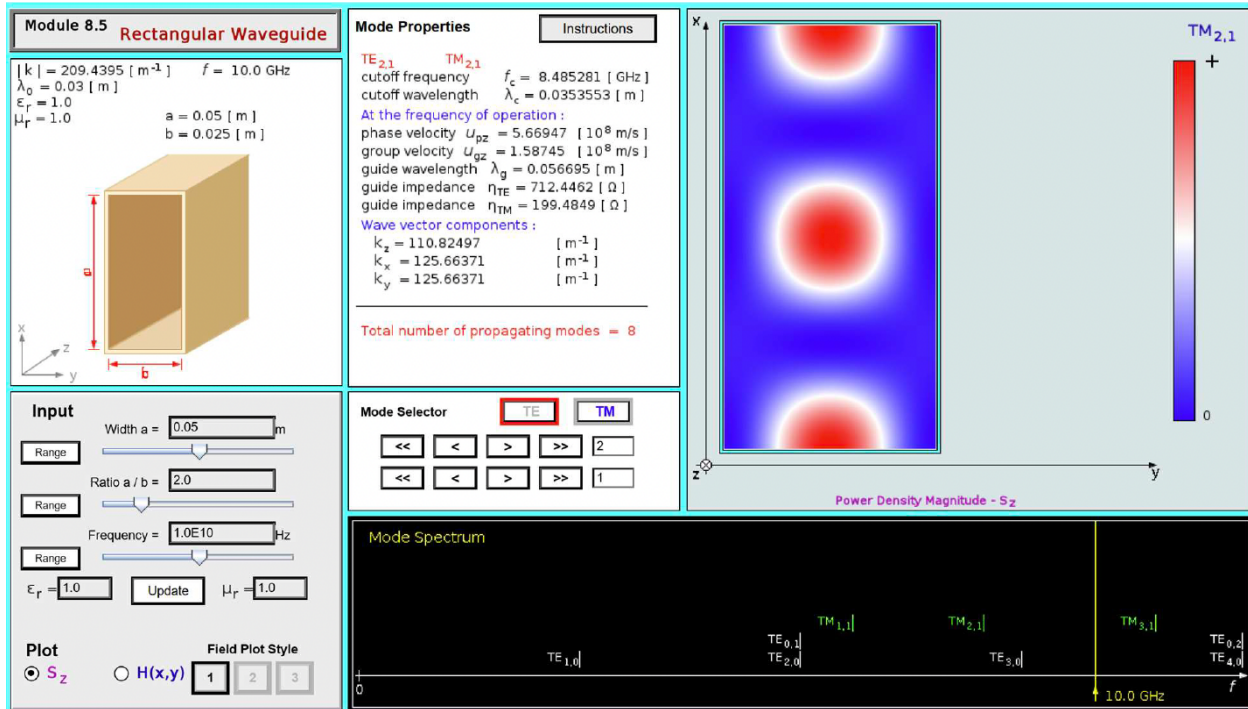


Figure 3.6 - Simulation of the  $TM_{2,1}$  mode for the power component  $S_z$

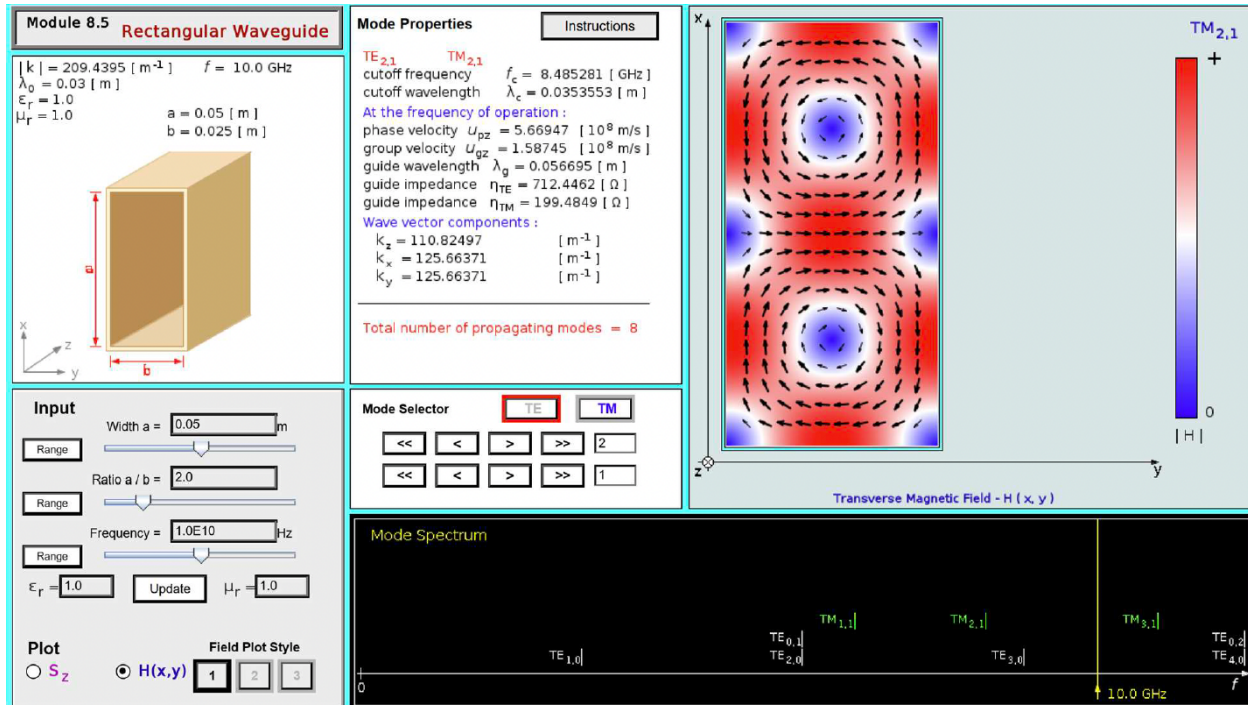


Figure 3.7 - Simulation of the  $TM_{2,1}$  mode for  $H(x,y)$

## Discussion:

### Part 1 – Dispersion Relations and Mode Identification

The dispersion curves generated for the first seven propagating modes clearly demonstrate the high-pass behaviour of the rectangular waveguide. Each mode begins propagating once the operating frequency exceeds its cutoff frequency  $f_c$ , and this is reflected in the dispersion figure by each  $\beta(f)$  curve starting at a different point before rising with frequency. Because

$$\beta(f) = \frac{2\pi}{c} \sqrt{f^2 - f_c^2},$$

modes with low  $f_c$  (such as  $TE_{10}$ ) rise sharply, while higher-order modes begin propagating later and grow more gradually.

The plot also shows pairs of curves that are identical and lie directly on top of each other. These correspond to degenerate TE/TM mode pairs, such as  $TE_{11}/TM_{11}$  and  $TE_{21}/TM_{21}$ . These modes appear the same in the dispersion plot because they share the exact same cutoff frequency, arising from the fact that they have the same transverse wavenumber combination

$$\left(\frac{m\pi}{a}\right)^2 + \left(\frac{n\pi}{b}\right)^2.$$

Since the cutoff frequency and propagation constant depend solely on this combination and not on whether the mode is TE or TM, their dispersion curves are identical even though their field patterns differ.

Using the cutoff frequencies taken from the simulation, exactly seven propagating modes exist below 10 GHz, matching theory and confirming the tool's accuracy.

### Part 2 – $TE_{10}$ Mode Field and Power Distributions

At the operating frequency of 10 GHz, the  $TE_{10}$  mode's simulated fields closely match theoretical predictions. The electric-field magnitude displays a single half-wave variation along the  $x$ -direction and no variation along  $y$ , consistent with

$$E_y \propto \sin\left(\frac{\pi x}{a}\right).$$

This pattern is clearly visible in the simulator's colour map, where the electric field peaks at the center and vanishes at the PEC walls.

The corresponding power-density plot  $S_z(x, y)$  confirms that the strongest energy flow occurs where both  $E_y$  and  $H_x$  reach maximum values. Power naturally drops to zero near the walls, reflecting the boundary condition that forces the tangential electric field to vanish. The simulated values of guide wavelength and TE-mode impedance agree closely with hand calculations, validating both the analytical model and the simulation.

## Part 3 – Degenerate Modes: Field Behaviour and Power Density

Degenerate modes have identical cutoff frequencies but different field patterns. The simulation of  $TE_{11}/TM_{11}$  and  $TE_{21}/TM_{21}$  illustrates this clearly. The dispersion curves for each pair overlap perfectly because their cutoff frequencies depend only on the transverse wave number pair  $(m, n)$ . Thus, TE and TM modes with the same indices will always have identical  $\beta(f)$ , regardless of how their fields look.

However, their power-density maps differ significantly. TE modes satisfy  $E_z = 0$  while TM modes satisfy  $H_z = 0$ , and this difference in boundary conditions results in different transverse field distributions through Maxwell's curl relations. As a result, the spatial shapes, nodal lines, and vector orientations of the fields differ between TE and TM modes with the same  $(m, n)$ .

Even though degenerate modes share the same cutoff frequency and therefore the same  $\beta(f)$ , they do not share the same power-density distribution because

$$S_z = \frac{1}{2} \Re\{E_y H_x^*\}$$

depends on the specific electric and magnetic field components. TE and TM modes enforce different PEC boundary conditions (Neumann for TE, Dirichlet for TM), which results in fundamentally different field orientations and magnitudes. These differences lead to distinct power-flow patterns, even though the dispersion relation is identical.

This explains why  $TE_{11}$  and  $TM_{11}$  appear identical on the dispersion plot but exhibit different energy-flow structures in the simulator.

## Conclusion:

This assignment demonstrated how electromagnetic modes behave within a rectangular waveguide and how theoretical predictions compare with numerical simulations. By determining the cutoff frequencies and generating dispersion relations for the first seven propagating modes, it became clear that the waveguide functions as a high-pass structure: only modes whose cutoff frequencies lie below the 10 GHz operating point are capable of propagation. The dispersion curves confirmed that the  $TE_{10}$  mode is the dominant mode and that higher-order modes propagate only when the operating frequency is sufficiently above their respective cutoffs. The simulations showed excellent agreement with analytical expectations, validating both the dispersion relation

$$\beta(f) = \frac{2\pi}{c} \sqrt{f^2 - f_c^2}$$

and the computed cutoff frequencies.

The field and power-density visualizations for the  $TE_{10}$  mode further reinforced the theoretical model. The simulator's  $E(x, y)$  distribution exhibited the expected sinusoidal dependence across the waveguide width and zero tangential electric field at the PEC boundaries. Likewise, the power-density map confirmed that energy flow is concentrated toward the center of the guide where the magnitudes of the transverse fields are highest. The excellent agreement between simulated and calculated values of  $\lambda_g$  and  $\eta_{TE}$  confirmed the consistency of Maxwell's equations with the numerical module.

A key goal of the assignment was to understand the behaviour of degenerate modes. The overlapping dispersion curves of  $TE_{11}/TM_{11}$  and  $TE_{21}/TM_{21}$  illustrated that degenerate modes share identical cutoff frequencies and therefore have the same dispersion relation. This occurs because the cutoff frequency depends only on the transverse wavenumber combination

$$\left(\frac{m\pi}{a}\right)^2 + \left(\frac{n\pi}{b}\right)^2,$$

which is the same for both TE and TM modes of equal  $(m, n)$ . However, the assignment also required explaining why their power-density distributions differ even though their dispersion does not, and the simulations made this distinction clear. Power density depends on the local interaction of electric and magnetic field components,

$$S_z = \frac{1}{2} \Re\{E_y H_x^*\},$$

and therefore on the specific field structure of each mode. Because TE modes satisfy  $E_z = 0$  and TM modes satisfy  $H_z = 0$ , the transverse fields generated through Maxwell's curl equations

differ between the two families. As a result, even though degenerate modes propagate with the same phase and group velocities, their internal electric-field patterns, magnetic-field orientations, and energy-flow distributions are distinct. The simulator's field maps confirmed these differences visually.

Overall, the assignment successfully demonstrated how analytical solutions, boundary conditions, and numerical simulation combine to give a complete understanding of waveguide behaviour. The comparison of TE and TM modes, the examination of dispersion, and the identification of degenerate-mode behaviour all reinforce the fundamental principles of electromagnetic propagation in guiding structures.

# Flow Diagram:

1. Initialize and clear workspace
  - 1.1 Clear all variables
  - 1.2 Close all figures
  - 1.3 Reset the command window
2. Define physical constants and geometry
  - 2.1 Set speed of light  $c = 3 \times 10^8$
  - 2.2 Set waveguide width  $a = 0.05$  m
  - 2.3 Set waveguide height  $b = 0.025$  m
3. Create frequency sweep
  - 3.1 Generate 2000 points from 0 to 10 GHz
  - 3.2 Store them in vector  $f$
4. Define waveguide modes
  - 4.1 List all modes with:
    - A label ("TE10", etc.)
    - Longitudinal index  $m$
    - Transverse index  $n$
5. Compute cutoff frequencies
  - 5.1 Extract all m-indices
  - 5.2 Extract all n-indices
  - 5.3 Compute cutoff for each mode:
$$f_c = \frac{c}{2} \sqrt{\left(\frac{m}{a}\right)^2 + \left(\frac{n}{b}\right)^2}$$
  - 5.4 Store all cutoff frequencies
6. Group degenerate modes
  - 6.1 Identify unique cutoff frequencies using MATLAB's `unique()`
  - 6.2 Group modes that share the same cutoff value
  - 6.3 Join labels of grouped modes into combined legend names
7. Apply colours
  - 7.1 Define custom RGB values
  - 7.2 Assign one color per degenerate group

## 8. Prepare dark-mode plotting environment

- 8.1 Create figure with black background
- 8.2 Create axes with dark grey background
- 8.3 Set tick-label and axis-label colors to white
- 8.4 Turn on grid, hold, and box

## 9. Compute and plot $\beta(f)$ for each group

For each group:

- 9.1 Extract that group's cutoff frequency
- 9.2 Initialize  $\beta(f)$  with NaN
- 9.3 Identify valid frequencies  $f > f_c$
- 9.4 Compute the propagation constant:  
$$\beta = \frac{2\pi}{c} \sqrt{f^2 - f_c^2}$$
- 9.5 Plot frequency vs  $\beta$
- 9.6 Store plot handle for legend

## 10. Add plot labeling

- 10.1 Label y-axis as "Frequency (GHz)"
- 10.2 Label x-axis as " $\beta$  (rad/m)"
- 10.3 Add descriptive title
- 10.4 Set axis font sizes and line thickness

## 11. Adjust axes limits

- 11.1 Set frequency axis from 0 to 10 GHz
- 11.2 Determine maximum  $\beta$  across all groups
- 11.3 Add 5% headroom to  $\beta$ -axis

## 12. Add legend

- 12.1 Use stored plot handles
- 12.2 Display grouped mode names
- 12.3 Set legend font color to white

## Code:

```
clear; close all; clc;

%% Constants and geometry
c = 3e8;      % speed of light
a = 0.05;     % width
b = 0.025;    % height

%% Frequency range
f = linspace(0,10e9,2000);

%% Mode list: {Label, m, n}
modes = {
    'TE10', 1,0;
    'TE01', 0,1;
    'TE20', 2,0;
    'TE11', 1,1;
    'TM11', 1,1;
    'TE21', 2,1;
    'TM21', 2,1;
    'TE30', 3,0
};

%% Compute cutoff frequencies
mvals = cell2mat(modes(:,2));
nvals = cell2mat(modes(:,3));
```

```
fc = (c/2) * sqrt((mvals./a).^2 + (nvals./b).^2);
```

```
%% Group degenerate modes
```

```
[unique_fc,~,idx] = unique(fc);
```

```
nGroups = length(unique_fc);
```

```
groups = cell(nGroups,1);
```

```
labels = cell(nGroups,1);
```

```
for g = 1:nGroups
```

```
    groupModes = modes(idx==g,1);
```

```
    labels{g} = strjoin(groupModes,' & '');
```

```
    groups{g}.fc = unique_fc(g);
```

```
end
```

```
%% Neon color palette
```

```
colors = [
```

```
    1.00 0.25 0.25; % red
```

```
    0.25 0.75 1.00; % blue
```

```
    0.40 1.00 0.40; % green
```

```
    1.00 0.70 0.20; % orange
```

```
    0.90 0.45 1.00; % purple
```

```
    0.30 1.00 0.85; % teal
```

```
    1.00 0.30 0.60 % magenta
```

```
];
```

```
%% Prepare figure
```

```

figure('Color',[0.10 0.10 0.10], 'Position',[100 100 900 550]);
axes('Color',[0.15 0.15 0.15], 'XColor','w', 'YColor','w', ...
'FontSize',11, 'LineWidth',1.2);
hold on; grid on; box on;

%% Plot beta vs frequency (axes swapped)
plotHandles = gobjects(nGroups,1);

for g = 1:nGroups
    fcg = groups{g}.fc;
    beta = nan(size(f));
    valid = f > fcg;
    beta(valid) = (2*pi/c) * sqrt(f(valid).^2 - fcg.^2);

    % SWAPPED AXES: plot beta on x-axis, f(GHz) on y-axis
    plotHandles(g) = plot(beta, f/1e9, 'LineWidth', 2.3, ...
        'Color', colors(g,:));
end

%% Labels and title
xlabel('\beta (rad/m)', 'FontSize', 13, 'Color','w');
ylabel('Frequency (GHz)', 'FontSize', 13, 'Color','w');
title('Dispersion Curves (f vs \beta) for Rectangular-Waveguide Modes', ...
'FontSize', 15, 'Color','w');

%% Axes limits
ylim([0 10]); % now vertical axis is frequency

```

```
maxBeta = max(arrayfun(@(fcg) ...
    max((2*pi/c) * sqrt(f(f>fcg).^2 - fcg.^2)), unique_fc));
xlim([0 maxBeta * 1.05]);

%% Legend
legend(plotHandles, labels, 'TextColor','w', 'Location','southeast);
```

## References

F. Ulaby, "Module 8.5." University of Michigan, Dept. of EECS. [Online]. Available: [https://em8e.eecs.umich.edu/jsmmodules/ch2/mod2\\_3.html](https://em8e.eecs.umich.edu/jsmmodules/ch2/mod2_3.html). Accessed on: November 26, 2025.

Schriemer, H. (2025). *ELG3106 Assignment 5: Modes in rectangular waveguides*

Schriemer, H. (2025). *Module 8: Waveguides (ELG3106 – Electromagnetic Engineering)*